*Mon. Not. R. astr. Soc.* (1990) **243,** 133–143

# Alternatives to the Press–Schechter cosmological mass function

J. A. Peacock
*Royal Observatory, Blackford Hill, Edinburgh EH9 3HJ*

A. F. Heavens
*Department of Astronomy, University of Edinburgh, Royal Observatory, Blackford Hill, Edinburgh EH9 3HJ*

Accepted 1989 August 30. Received 1989 August 30; in original form 1989 July 24

**SUMMARY**

We investigate the validity of the Press–Schechter formalism for calculating the mass distribution function, $f(M)$, of the bound objects which condense out of a primordial density perturbation field. We give a revised analysis, which automatically has the correct normalization and accounts explicitly for the mass in underdense regions. The resulting $f(M)$ depends on the form of the filter function chosen; in general this method predicts *more* low-mass objects than the Press–Schechter formalism. We also consider the effects of identifying density maxima as the sites of proto-objects. This predicts an $f(M)$ with a different shape, but again with a low-mass power-law tail which lies above the Press–Schechter result, unless a very large mass is assigned to each peak.

Our method allows additional constraints to be added to govern the formation of certain classes of object. As an illustration, we calculate a mass function for galaxies, using the criterion that an object must have been able to cool in the time between its collapse epoch and the present. This produces a mass-dependent overdensity threshold which can reduce the relative abundance of low-mass objects considerably, providing a qualitative explanation for the form of the galaxy luminosity function.

## 1 INTRODUCTION

The mass function for bound objects is an important quantity in cosmology. In principle, this distribution can distinguish powerfully between different candidate theories for galaxy formation, including such fundamental issues as whether or not the initial perturbations were Gaussian (see e.g. Lucchin & Matarrese 1988). Unfortunately, it has long been clear that the non-linear phases of collapse and merging are sufficiently complex to preclude a completely analytic approach to this problem. Nevertheless, the importance of the issues involved means that even an approximate treatment is of value, especially in extrapolating the results of numerical studies to new parameter regimes and to rare objects.

An early landmark in this field was set by Press & Schechter (1974; PS), who gave a prescription for estimating the mass distribution function for a hierarchical Gaussian density field. Interest in this formalism has recently been strong, motivated by numerical simulations which appear to show good agreement with the PS result (Efstathiou *et al.* 1988; Carlberg & Couchman 1989). These results have led to diverse investigations using the PS formalism, including the formation epoch of the first massive galaxies (and hence quasars; Efstathiou & Rees 1988) and the expected gravitational-lens properties of a Cold Dark Matter universe (Narayan & White 1988).

The PS analysis covers most situations where the power spectrum of initial density perturbations contains power at a wide range of wavenumbers. The limitation to Gaussian fields may appear rather restrictive, but this is simply a consequence of assuming uncorrelated phases for the various Fourier components of the density field (via the central limit theorem). Thus, although it is quite possible to analyse non-Gaussian density fields (see Lucchin & Matarrese 1988 for application to the mass function), Gaussian fields arise with sufficient generality to be much the most important case. Our understanding of Gaussian random fields have advanced since the work of PS, notably with the recent surge of interest in density maxima as sites for potential collapsed objects [Peacock & Heavens 1985; Bardeen *et al.* 1986 (BBKS)]. The purpose of this paper is thus to review the PS formalism and attempt to understand why it works so well in practice, despite the fact that the analysis contains several features long recognized as unsatisfactory. We consider modifications of three kinds: (i) accounting correctly for the fate of material in underdense regions, which was not treated by PS; (ii) incorporation of the recent results on density peaks and (iii) considering a simple model for the effects of cooling, to estimate the mass function for 'luminous' objects.

## 2 MODIFICATIONS OF THE PS FORMALISM

### 2.1 Basics

We begin by outlining the basic PS result. The critical concept is that of *filtering* the initial density field $\delta(\mathbf{x}) \equiv \delta\rho/\rho$.

A large class of density fields will be dominated by fluctuations on some small physical length scale, which collapse non-linearly and then cluster together/merge to produce a more massive member of the hierarchy. The PS assertion (which we adopt) is that the location and properties of these objects can be estimated by an artificial smoothing (or filtering) of the initial linear density field. If the filter function has some characteristic length $R_f$, then the typical size of filtered fluctuations will be $\sim R_f$ and they can be assigned a mass $M \sim \rho_0 R_f^3$. The exact analytic form of the filter function is arbitrary and is often taken to be a Gaussian for analytic convenience. The implicit assumption has been that different choices of 'reasonable' filter functions (lacking large side-lobes or $k$-space wings) would yield rather similar results. This turns out not to be the case, as we shall see below.

The argument now proceeds in integral terms. For a given $R_f$, the probability that a given point lies in a region with $\delta > \delta_c$ (the critical overdensity for collapse) is

$$p(\delta > \delta_c \,|\, R_f) = \tfrac{1}{2}\left[1 - \operatorname{erf}\left(\frac{\delta_c}{\sqrt{2}\,\sigma(R_f)}\right)\right], \tag{1}$$

where $\sigma(R_f)$ is the linear rms in the filtered version of $\delta$. The PS argument now takes this to be proportional to the probability that a given point has ever been processed through a collapsed object of scale $> R_f$. This assumes that the only objects which exist at a given epoch are those which have just collapsed; if a point has $\delta > \delta_c$ for a given $R_f$, then it will have $\delta = \delta_c$ when filtered on some larger scale and will be counted as an object of the larger scale. The problem with this argument is that half the mass remains unaccounted for; this was amended by PS simply by multiplying the probability by a factor 2.

This integral probability is related to the mass function $f(M)$ [defined such that $f(M)\,dM$ is the comoving number density of objects in the range $dM$] via

$$Mf(M)/\rho_0 = |\,dp/dM\,|, \tag{2}$$

where $\rho_0$ is the total comoving density. Thus,

$$f(M) = \frac{2\delta_c}{\sqrt{2\pi}\,\sigma}\,\frac{\rho_0}{M^2}\left|\frac{d\ln\sigma}{d\ln M}\right|\exp(-\tfrac{1}{2}\delta_c^2/\sigma^2). \tag{3}$$

The factor of 2 'fudge' has long been recognized as the crucial weakness of the PS analysis. What one has in mind is that the mass from lower density regions accretes on to collapsed objects, but it does not seem correct for this to cause a doubling of the total number of objects.

## 2.2 The cloud-in-cloud problem

To improve on the PS analysis, it is necessary to treat the points with $\delta < \delta_c$ explicitly. The real problem with the above discussion is that it is local; it takes no account of how the fields at several different $R_f$ values are related to each other. Consider a single field point and think of the trajectory taken by $\delta$ as a function of $R_f$; for a set of very widely spaced $R_f$ values, the fields will be essentially independent samples of Gaussians with the appropriate variance $\sigma^2(R_f)$. Now, if $\sigma(R_f) \to \infty$ as $R_f \to 0$ (i.e. we are dealing with a hierarchical density field that lacks a low-wavelength cut-off), then it is certain that $\delta$ will exceed $\delta_c$ on some small scale. The important question is then to find the *largest* filter value for which $\delta$ is equal to the threshold, known as the first upcrossing of the process $\delta(R_f)$. This finds the largest mass which has collapsed about that point by the present epoch, destroying in the process any sub-structure.

It is easy to write down a framework for calculating the probability distribution of these upcrossing points, as follows

$$p(>R_f) = p_G(\delta > \delta_c) + \int_{-\infty}^{\delta_c} \frac{dp_G}{d\delta}\, p_{up}(\delta_c, \delta)\, d\delta, \tag{4}$$

where $p_G$ is the Gaussian distribution. This says we should divide points at $R_f$ into two classes. Those with $\delta > \delta_c$ clearly have $\delta = \delta_c$ for some larger filter, and are therefore associated with objects of scale $> R_f$. For all points below the threshold, we expect that there is some probability, $p_{up}$, that subsequent filterings might at some point result in having $\delta$ above the threshold; if we can calculate this, the problem is solved.

This prescription has the important property that it is automatically normalized. From the argument given earlier, it is clear that $p_{up} \to 1$ as we go to very small scales. The PS argument corresponds to taking only the first term in the above equation and doubling it. It is far from obvious that the two terms are equal, so one might doubt the validity of the PS factor 2; we shall see that such doubts are generally well founded.

## 2.3 Survival probabilities

The problem of calculating the upcrossing probabilities is mathematically rather nasty, due to the correlations between $\delta$ at various $R_f$ values. Consider a pair of density fields at a given point, $\delta_1$ and $\delta_2$, and define the dimensionless amplitude $\nu$

$$\nu \equiv \frac{\delta(R_f)}{\sigma(R_f)}. \tag{5}$$

Taking fields $\nu_1$ and $\nu_2$ in terms of their respective rms values, we have

$$\frac{dp(\nu_2 \,|\, \nu_1)}{d\nu_2} = \frac{1}{[2\pi(1-\varepsilon^2)]^{1/2}} \exp\left[-\frac{(\nu_2 - \varepsilon\nu_1)^2}{2(1-\varepsilon^2)}\right], \tag{6}$$

where we have adopted the notation used by BBKS

$$\varepsilon \equiv \frac{\sigma_{0h}^2}{\sigma_{01}\sigma_{02}}, \tag{7}$$

$$\sigma_{ji}^2 \equiv \frac{V}{(2\pi)^3} \int k^{2j} F_i^2(k)\,|\,\delta_k|^2\, d^3k, \quad i = 1, 2; \tag{8}$$

$$\sigma_{jh}^2 \equiv \frac{V}{(2\pi)^3} \int k^{2j} F_1(k) F_2(k)\,|\,\delta_k|^2\, d^3k. \tag{9}$$

As usual in this subject, the statistics of the field are specified by a series of moments over the power spectrum $|\delta_k|^2$, filtered by the appropriate $F(k)$ factors (we use the Fourier transform convention which introduces an arbitrary normalization volume, $V$).

Analogous expressions may be derived for the case of several coupled fields. However, the integration over such a distribution to find the probability that all the filtered fields are lower than the threshold is not, in general, straightforward. Certainly, taking the limit of such a procedure for an infinite number of (closely correlated) fields is not an attractive prospect, and we have therefore adopted a more intuitive approach, as follows. Once the field has been filtered by a large amount, the result is essentially independent of the original value and the probability of exceeding the threshold is just the unconstrained value; the same is true for all subsequent filterings where $R_f$ changes by a further large factor. The *survival probability* (the probability of always remaining below the threshold; $p_s \equiv 1 - p_{up}$) is then the product over these independent fields,

$$p_s(\delta_c) = \prod_i p_i(\delta < \delta_c). \tag{10}$$

Imagine a sequence of fields where we progressively reduce the spacing in $R_f$; the above relation will clearly hold until the separation is a factor of order unity in $R_f$. We will then have encountered the analogue of a coherence length in log $R_f$.

This suggests the following simple ansatz for the survival probability,

$$\ln p_s = \int_0^\infty \ln p(\delta < \delta_c \,|\, R_f) \frac{d \ln R_f}{\Delta}, \tag{11}$$

where $\Delta$ is the critical increment in $\ln R_f$ for effective independence (at this stage, $\Delta$ is simply a parameter to be determined, and will depend on the power spectrum). Note that this expression contains the unconditional probability $p(\delta < \delta_c \,|\, R_f)$, rather than $p(\delta < \delta_c \,|\, R_f, \delta_i)$, so that $p_s$ is independent of $\delta_i$. This cannot be precisely true, but does seem to be a good approximation (see below).

We can infer the value of $\Delta$ as follows. Consider the set of all points which have $\delta < 0$ for some value of $R_f (= R_0)$; the above argument suggests that the probability that they will remain underdense for all subsequent filterings up to $R_f = R_1$ is given by $p_s(0) = (R_0/R_1)^{(\ln 2)/\Delta}$ – i.e. $p_s$ falls as a power law in $R_f$. We can now use equation (6) to find $\Delta$ by evaluating $d \ln p_s / d \ln R_f$ at $R_1 = R_0$. Here, we calculate what fraction of underdense points are scattered above the $\delta = 0$ threshold by an infinitesimal amount of filtering. The problem is simplified at this stage as we do not need to take into account the results of any configurations intermediate between the initial and final filterings. Thus, we use the initial rate of change of the conditional probability to find the slope of the power law determined by equation (11). For Gaussian filtering $[F(k) = \exp(-\tfrac{1}{2}k^2 R_f^2)]$, we have

$$\varepsilon \simeq 1 - \frac{R_0^4}{2}\left(\frac{\sigma_2^2}{\sigma_0^2} - \frac{\sigma_1^4}{\sigma_0^4}\right)[\ln(R_1/R_0)]^2 \equiv 1 - \tfrac{1}{2} g^2 [\ln(R_1/R_0)]^2. \tag{12}$$

Inserting this into equation (6) and integrating over $\nu_1$ and $\nu_2$, the upscattering probability can be written [to first order in $\ln(R_1/R_0)$] as

$$p(\nu_2 > 0 \,|\, \nu_1 < 0) = 2\,\frac{g \ln(R_1/R_0)}{2\pi} \int_0^\infty \int_x^\infty e^{-y^2/2}\, dy\, dx = \frac{g \ln(R_1/R_0)}{\pi} \tag{13}$$

[reversing the order of integration, and using $p(\nu_1 < 0) = \tfrac{1}{2}$ initially]. Hence, we obtain an expression for the parameter $\Delta$,

$$\Delta = \frac{\pi \ln 2}{R_f^2}\left[\frac{\sigma_2^2}{\sigma_0^2} - \frac{\sigma_1^4}{\sigma_0^4}\right]^{-1/2}. \tag{14}$$

It is straightforward in principle to derive the corresponding expressions for other filter functions. In general, one must find the analogue of the function $g$ and set $\Delta = (\pi \ln 2)/g$. This will involve $k$-space integrals over derivatives with respect to $R_f$ of the $k$-space filter function. Gaussian filtering is analytically convenient, in that these integrals reduce to moments of the power spectrum. We shall therefore give results for Gaussian filtering only in what follows. However, we emphasize that the analysis is general and can, in principle, be applied to any differentiable filter function.

This completes the prescription needed to evaluate survival probabilities for field points. It should be immediately clear that this may in general lead to results rather different from the original PS formula. Differentiate the fundamental equation (4) to obtain the differential distribution of $R_f$ values; in the limit of small $R_f$, where $p_{up} \to 1$, this becomes simply

$$\frac{dp}{dR_f} = \frac{1}{2}\frac{dp_{up}}{dR_f}. \tag{15}$$

As the survival probability only goes to zero as a slow power law $p_s \propto R_f^{(\ln 2)/\Delta}$, the possibility is raised that this term might tend to dominate the mass function for small $R_f$. We will see below that this is indeed the case; this formalism will usually predict more low-mass objects than the original PS formula.

### 2.4 Sharp *k*-space filtering

It is clear that this ansatz will not work in all cases. When the first derivative of $k$-space filter function with respect to $R_f$ does not exist, it is possible to have

$$\varepsilon = 1 - O \ln(R_1/R_2), \tag{16}$$

and our procedure will fail. The main example of this case is sharp truncation in $k$-space. This has been investigated recently in the context of the PS model by Bond *et al.* (in preparation 1989) and has some appealing properties. Crucially, the field in this case executes a random walk from $\delta = 0$ at $R_f = \infty$; each new slice of $k$-space added is independent. In this case, one can use the following argument to deduce the survival probability (Chandrasekhar 1943). For $\delta < \delta_c$ the probability density of points which have upcrossed at a larger $R_f$ must, by the symmetry of the random walk, simply be the reflection in the threshold of those points above the threshold. The upcrossing probability is then

$$p_{up} = \frac{\exp[-(\delta - 2\delta_c)^2/2\sigma^2]}{\exp(-\delta^2/2\sigma^2)}, \tag{17}$$

and the total probability of upcrossing is

$$\int_{-\infty}^{\delta_c} \frac{dp_G}{d\delta} p_{up}(\delta_c, \delta)\, d\delta = \frac{1}{\sqrt{2\pi}\sigma}\int_{-\infty}^{\delta_c} \times \exp[-(\delta - 2\delta_c)^2/2\sigma^2]\, d\delta$$

$$= p_G(>\delta_c). \tag{18}$$

Miraculously, this is simply the original PS term; the analysis by Bond *et al.* supplies the PS factor of 2 without needing to cheat. However, as most filter functions that one might want to consider *are* differentiable, this is a rather special case.

## 3 RESULTS

### 3.1 Power-law spectra

These results can be cast in a reasonably simple form for power-law power spectra, $|\delta_k|^2 \propto k^n$. For Gaussian filtering in $D$ dimensions, we have

$$\frac{\sigma_m^2(R_f)}{\sigma_m^2(R_0)} = \left(\frac{R_0}{R_f}\right)^{n+2m+D}, \tag{19}$$

$$\frac{R_*}{R_f} = \left(\frac{2D}{n+D+2}\right)^{1/2}, \tag{20}$$

$$\gamma = \left(\frac{n+D}{n+D+2}\right)^{1/2}, \tag{21}$$

$$\varepsilon = \left(\frac{2R_0R_f}{R_f^2+R_0^2}\right)^{(n+D)/2}, \tag{22}$$

$$\Delta = \pi \ln 2\left[\frac{n+D}{2}\right]^{-1/2}. \tag{23}$$

If we define

$$\nu \equiv \frac{\delta_c}{\sigma_0(R_f)}, \tag{24}$$

then we have the limiting behaviour

$$p_s(\nu) \sim \nu^{[2/(n+D)]^{1/2}/\pi}, (\nu \ll 1). \tag{25}$$

Fig. 1 shows the results of our procedure for power-law spectra, in the form of $P(>\nu)$ curves. This shows explicitly the two terms in equation (4), and their sum. These are for random fields in three dimensions, but the above equations show that the result depends only on $n+D$. The clear result in all cases is that the second term in equation (4) is generally smaller than the first. For large $\nu$, we have exactly half the PS result.

Fig. 2 now shows these results in differential form, $dp/d\ln\nu$. As from equation (2),

$$M^2 f(M)/\rho_0 = \left(\frac{dp}{d\ln\nu}\right)\left(\frac{d\ln\nu}{d\ln M}\right), \tag{26}$$

and the second term on the right is a constant for power-law spectra, we see that these plots are identical in shape to $M^2 f(M)$. It is worth emphasizing the advantage of writing the mass function in this form. It allows us to include, for example, a criterion on collapse from cooling (see Section 5) or mass-dependent biasing, by appropriate calculation of the second term on the right-hand side.

The pronounced difference in low-mass slope between Gaussian and sharp filtering is immediately apparent in these diagrams. The PS formula has $P(<\nu) \propto \nu$ for $\nu \ll 1$, whereas in our prescription the survival probability $p_s$ dominates. In three dimensions, with $M \propto R_f^3$, this leads to a low-mass slope in our prescription of

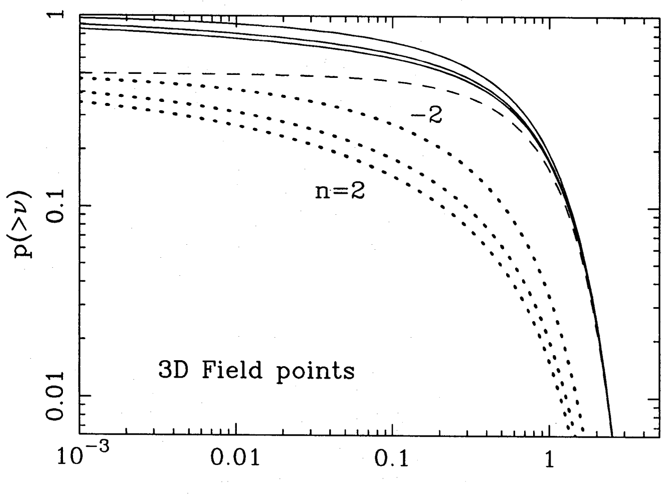


**Figure 1.** The integral probability distribution for first upcrossing points of a Gaussian-filtered three-dimensional random Gaussian field. The filter radius of upcrossing is specified in terms of $\nu \equiv \delta_c/\sigma(R_f)$. Three curves are shown; the fraction of mass which lies above the threshold at a given scale (dashed); the fraction which lies below the threshold, but lies above the threshold on some larger scale (dotted); and the total (solid). The first fraction is always the larger, and corresponds to half the PS result.

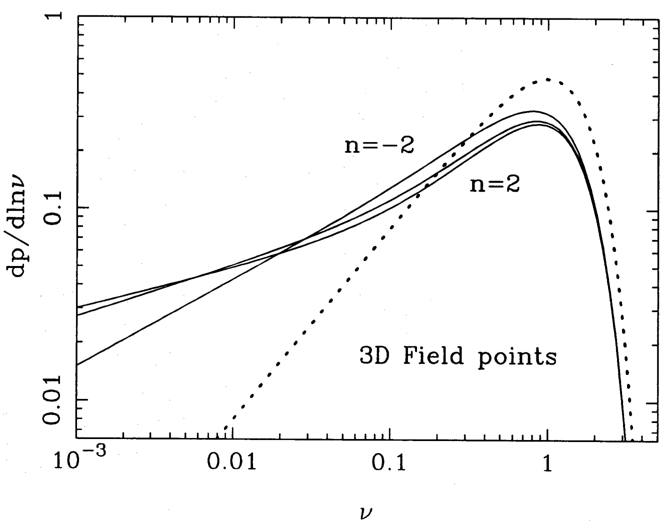


**Figure 2.** The total results of Fig. 1 in differential form, $dp/d\ln\nu$. Since $M^2f(M)/\rho_0 = (dp/d\ln\nu)(d\ln\nu/d\ln M)$, these plots are identical in shape to the multiplicity function; $M^2f(M)/\rho_0$ gives the fraction of the mass of the universe carried by objects in unit range of $\ln M$. The PS result (which is the same for all spectra) is shown dotted. Our prescription predicts more low-mass objects in all cases.

$$M^2 f(M) \propto M^{[(n+3)/18]^{1/2}/\pi}, \tag{27}$$

compared to the PS result

$$M^2 f(M) \propto M^{(n+3)/6}. \tag{28}$$

Hence there are more low-mass objects provided that $n > -2.8$. For $n = -2$, the difference in slopes is 0.07, for $n = -1$ it is about 0.2.

The solution to the PS problem then turns out to be rather different from that originally envisaged, except for rather special choices of filtering. Before advocating these mass functions as an improvement on the PS formula, however, there are further modifications to consider.

## 4 THE PS FORMALISM IN TERMS OF DENSITY MAXIMA

Another area of incompleteness in the original PS argument is its lack of detail over exactly how overdense regions are related to bound proto-objects. This shortcoming has been addressed by the recent work on density peaks in Gaussian fields. Regarding these as the sites of potential collapsed objects suggests some modifications of the PS formalism, as follows.

In BBKS notation, the number density of peaks in a Gaussian field in $D$ dimensions is

$$n_{\rm pk}\, d\nu = \frac{1}{(2\pi)^{(D+1)/2} R_*^D} \, e^{-\nu^2/2} G(\gamma, \gamma\nu)\, d\nu, \tag{29}$$

where $\nu \equiv \delta/\sigma_0$, $R_* \equiv \sqrt{D}\, \sigma_1/\sigma_2$ and $\gamma \equiv \sigma_1^2/(\sigma_0 \sigma_2)$ in terms of $2i$th moments over the power spectrum, $\sigma_i^2$. The function $G$ is given by

$$G(\gamma, x_*) = \int_0^\infty F(x) \frac{\exp\left[ -\dfrac{1}{2} \dfrac{(x - x_*)^2}{(1-\gamma^2)} \right]}{[2\pi(1-\gamma^2)]^{1/2}}\, dx. \tag{30}$$

In one dimension, $F(x) = x$ (Rice 1954), whereas $F(x) = x^2 + \exp(-x^2) - 1$ in two dimensions (Bond & Efstathiou 1987). $F(x)$ is given for $D = 3$ by BBKS equations (A1.9) and (4.5).

A simple peak version of a mass function now suggests itself. On a scale $R_{\rm f}$, consider the fraction of mass associated with a peak above the threshold, $MN_{\rm pk}(>\nu)/\rho_0$, to give the integral mass probability distribution (where $M$ is the mean mass associated with peaks above threshold $\nu$ on a filter scale $R_{\rm f}$, and $N_{\rm pk}$ is the integral number density of peaks). If $M/R_*^3$ is a constant, then we obtain

$$f(M) = \frac{\nu}{M} n_{\rm pk}(\nu) \left( \frac{d \ln \nu}{d \ln M} \right), \tag{31}$$

which was given implicitly by Efstathiou & Rees (1988) and explicitly by Bond (1989). This peak $f(M)$ is very similar in form to the PS formula, modified only by the $G(\nu, \gamma\nu)$ factor. As this goes to a constant for $\nu \ll 1$, the numbers of low-mass objects cut-off no more abruptly than in the PS formula, which is in contradiction to an assertion by Lucchin & Matarrese (1988). Their result was arrived at by assuming the high-$\nu$ limit for $n_{\rm pk}$, which has $n_{\rm pk} \propto \nu^3 \exp(-\nu^2/2)$; however, for low masses $\nu \ll 1$, and their expression is thus invalid.

The physical basis for this analysis is that any material within a distance $\sim R_{\rm f}$ of a peak which has collapsed is assumed to be part of a system with mass at least $\sim \rho_0 R_{\rm f}^3$. This seems a better physical motivation than PS, but it shares the same deficiency that connected regions assigned a mass $M$ are not guaranteed to have the appropriate volume $\sim M/\rho_0$.

There is an interesting contrast between this formula and PS concerning the normalization of $f(M)$; the PS formalism automatically accounts for all the mass; the $M(R_{\rm f})$ relation simply fixes the number density of objects. For the case of peaks, the number density is determined, and only one choice of $M_{\rm pk}(R_{\rm f})$ will give a correct normalization. BBKS showed that the total density of peaks (of any $\nu$) was about $0.016 R_*^{-3}$, so we might hope for $M_{\rm pk} \simeq 63 \rho_0 R_*^3$. We now consider what this mass should actually be.

### 4.1 Mass estimates

There is a variety of choices for peak mass estimates. The simplest is the volume of the filter function $M = (2\pi)^{3/2} \rho_0 R_{\rm f}^3$ (as used by e.g. Efstathiou & Rees 1988). Here, we view the filtering process as producing the mean density within some volume; an object of size $\sim R_{\rm f}$ is expected to collapse when this mean overdensity reaches $\delta_{\rm c} \simeq 1$. Note that the collapse of this volume only requires the filtered $\delta > \delta_{\rm c}$ at *one* point – in this respect artificial and physical filtering differ markedly. This is certainly reasonable for a spherical top-hat filter and a spherically symmetric mass distribution ($\delta_{\rm c} = 1.69$ in this case).

The comparison with the spherical filter provides an alternative method of assigning a mass to peaks. In some sense, the equivalent sphere to (say) a Gaussian filter should be the sphere (of radius $R_{\rm sph}$) which produces the same rms as the applied filter of scale $R_{\rm f}$. In $k$-space, the Gaussian and spherical filters agree to second order in $k$ if $R_{\rm sph} = \sqrt{5} R_{\rm f}$. The volume of this sphere is

$$V = \frac{4\pi}{3} 5^{3/2} R_{\rm f}^3, \tag{32}$$

which is a factor 2.97 larger than $(2\pi)^{3/2} R_{\rm f}^3$. Although the detailed $R_{\rm sph}(R_{\rm f})$ relation for equal rms depends on the power spectrum, it is within 20 per cent of this factor for $n < 0.5$, and so there might be some justification for taking a uniformly larger mass.

An alternative viewpoint is that non-linear development of small-scale perturbations into collapsed objects may be thought of as acting in a sense like a genuine physical filter on the remaining linear portion of the power spectrum. This leads us to consider the problem of the density profile of a peak. Peacock & Heavens (1985) attempted to produce a peak mass estimate by modelling the peaks as triaxial spheroids, and estimating the volume of the region with $\delta > 0$. According to this prescription, there is a distribution of masses for a given $\nu$; however, we shall not be particularly interested in this distribution as any dispersion in mass at a given $R_{\rm f}$ will be dominated by the fact that we are considering a wide range in $R_{\rm f}$. The mean value of $\log M$ may be approximated (for values $0.5 \lesssim \gamma \lesssim 0.8$ of practical interest) by

$$M = \frac{2^{3/2}[(4\pi)/3]\rho_0 R_*^3}{[\gamma^3 + (0.9/\nu)^{3/2}]}. \tag{33}$$

For a spherical peak with quadratically varying overdensity, the bound mass is a factor $(5/3)^{3/2}$ larger than the above expression. Certainly, it may seem reasonable that low-$\nu$ peaks should have lower mass; peaks with $\nu \simeq 0$ will tend to sit in regions of larger scale underdensity (cancelling the small-scale overdensity), and hence the $\sim \rho_0 R_*^3$ of material, which initially surrounds the peak, may not be accreted following central collapse.

We shall not consider the effects of this specific mass estimate of $f(M)$ in detail. It is sufficient at present to note that, together with the earlier discussion, there may well be grounds for wanting to adopt a peak mass either smaller or larger than the strict $M = (2\pi)^{3/2}\rho_0 R_f^3$ relation; we shall see below that this can have important consequences for the mass function.

In passing, we should mention the relation of this discussion to the topic of the angular momentum acquired by a collapsed density maximum, which was studied by Heavens & Peacock (1988). In that paper, we showed that the median value of the dimensionless spin parameter, $\lambda$, scaled approximately as $\langle\lambda\rangle \simeq 0.08/\nu$ (this result is independent of the overdensity criterion used to define the peak boundary). We have now confirmed this dependence for low peaks down to $\nu = 0.01$. For the above mass estimates, we have $\nu \propto M^\alpha$, where $\alpha = (n+3)/6$ for the simple mass estimates, or $\alpha = (2n+6)/(3n+21)$ for the full peak mass estimate. If the effective spectral index on scales of galaxies is $n \simeq -2$, as would be expected in the CDM model (see Section 6), then $\alpha \simeq 0.15$ whatever mass estimate is used. Thus, objects with masses $\sim 10^{-7}\, M_c$ should be rotationally supported, where $M_c$ is the mass scale which is collapsing now, i.e. $\sigma(M_c) \simeq \delta_c$.

### 4.2 Survival probabilities and peaks

The previous section has shown that, generally, the fraction of mass associated with a peak on a given filtering scale will be small. In one dimension, the number density of all peaks is $(2\pi R_*)^{-1}$, which encloses a fraction

$$f_{pk} = (2\pi)^{-1/2}\frac{R_f}{R_*} = \left(\frac{3+n}{4\pi}\right)^{1/2} \tag{34}$$

for Gaussian filtering with $M = (2\pi)^{1/2}\rho_0 R_f$, and ignoring peak overlap. In three dimensions, the corresponding expression is

$$f_{pk} = 0.016 R_*^{-3}(2\pi)^{3/2} R_f^3 \simeq \left(\frac{n+5}{15}\right)^{3/2}. \tag{35}$$

These fractions are $\lesssim 0.5$ for power spectra of practical interest, so it is clearly vital to treat correctly the material which lies outside a peak on a given scale.

We can attack this problem in much the same way as we did for field points. Material which lies outside a peak on one scale can sometimes lie inside a peak on a larger filtering scale. For very low thresholds, the probability of this occurring clearly goes to unity. Thus, as with field points, we can write an expression which is automatically normalized

$$p(>R_f) = f_{pk}(\delta > \delta_c) + (1 - f_{pk})p_{up}. \tag{36}$$

The critical term $p_{up}$ is the analogue of the upcrossing probability; the probability that a point outside a peak will find itself inside one on some larger filtering scale. Following our previous reasoning, we again make the ansatz that $p_{up}$ may be estimated by saying that random fields should be effectively independent after some increment $\Delta$ in $\ln R_f$,

$$\ln[1 - p_{up}] = \int_0^\infty \ln[1 - f_{pk}(\delta > \delta_c \mid R_f)]\,\frac{d\ln R_f}{\Delta}. \tag{37}$$

The problem with this is that there is no reason to suppose that the appropriate value of $\Delta$ for this problem will be the same as the one we deduced for the case of field points. Indeed, we shall shortly see that they are in fact very different.

Filtering a random field may remove or create peaks, and almost all peaks will be lower as filtering reduces the variance of the field. Nevertheless, for a small amount of smoothing, almost all peaks will be at essentially the same positions and the number above a threshold will change only by a fractional amount of order $\delta R_f/R_f$. However, *all* these peaks will be more massive, due to the increase in $R_f$. Thus, to first order in $\delta R_f$, the only change in the fraction of mass which has been inside a peak is due to the mass swept up as the peaks 'bloat'.

We can now use the same trick as for field points. Consider an initial threshold of zero, and argue that the fraction of mass not associated with a peak must fall as some power law in $R_f$, the slope of which depends on $\Delta$. As we can find the initial rate of changing of this fraction through the above 'bloating' argument, the appropriate value of $\Delta$ may be deduced. If we call the fraction of mass that has ever been inside a peak $F_{pk}$, then we denote the fraction inside peaks above zero threshold on a given scale by $f_{pk}(0)$. The 'bloating' argument says that, in this initial case,

$$dF_{pk} = f_{pk}(0)D\frac{dR_f}{R_f}, \tag{38}$$

where $D$ is the number of dimensions. In terms of the fraction never inside a peak, the initial logarithmic rate of change of survival probability is

$$\frac{d\ln(1-F_{pk})}{d\ln R_f} = -\frac{Df_{pk}(0)}{1 - f_{pk}(0)}, \tag{39}$$

and as the ansatz for $p_{up}$ asserts that the left-hand side of this equation is always equal to $\ln[1 - f_{pk}(0)]/\Delta$, we obtain

$$\Delta_{pk} = -\frac{[1 - f_{pk}(0)]\ln[1 - f_{pk}(0)]}{Df_{pk}(0)}. \tag{40}$$

For the small values of $f_{pk}(0)$ that are typical in three dimensions, this tends to $\Delta_{pk} \simeq 1/3$, which is roughly an order of magnitude less than $\Delta_{field}$.

This is an amusingly crude argument, when one considers the complications of solving exactly for the probability of a point lying inside at least one set of peaks on many different filtering scales. Nevertheless, as we shall see, it does seem to work. The argument is designed to give the correct slope for $f(M)$ at very low masses; because $f(M)$ looks roughly like a power law with an exponential cut-off, it is therefore perhaps not so surprising that the overall shape can be constrained by this ansatz.

### 4.3 Results

We show the results of the above procedure for Gaussian-filtered power-law spectra in Fig. 3, in the form of $dp/d\ln\nu$. Both figures adopt the simple mass estimates ($\sqrt{2\pi}\rho_0 R_f$ for $D=1$, $(2\pi)^{3/2}\rho_0 R_f^3$ for $D=3$). Comparison with the field-point results shows that far fewer low-mass objects are now predicted. In one dimension, these peak $f(M)$ curves resemble the PS formula, although in three dimensions there are generally still more low-mass objects than predicted by PS.

It does seem reasonable that the peak $f(M)$ should predict fewer low-mass objects. In the field-point calculation, a point is assigned to mass $>M$ if it exceeds $\delta_c$ on that scale. As one point at $\delta_c$ corresponds to the collapse of a whole region, however, the field-point calculation will assign too few points to large systems, and thus overestimate the abundance of low-mass objects.

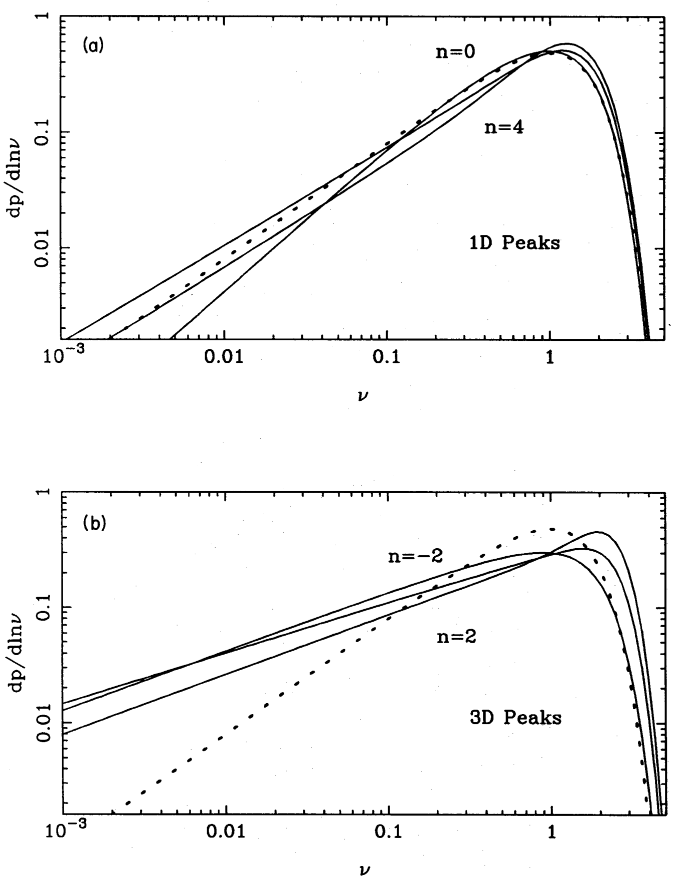


**Figure 3.** The mass functions for peaks in differential form, $dp/d\ln\nu$ (the analogue of Fig. 2 for field points). (a) In one dimension, (b) in three dimensions. Again, the PS result is shown dotted. Note that the numbers of low-mass objects predicted are lower than in the field-point case.

The precise slopes of these curves should not, however, be taken as having too much significance. The asymptotic behaviour resulting from $dp_{up}/dM$ is

$$M^2 f(M) \propto M^{-\ln[1-f_{pk}(0)]/(D\Delta)} = M^{f_{pk}(0)/[1-f_{pk}(0)]}, \tag{41}$$

which will change according to the mass estimate we use. For field points, the low-mass slope depended on the analytic form of the filter function. For peaks, this seems less important, but the question of the $M(R_f)$ relation (which is non-trivial for all but spherical top-hat filters) becomes crucial. As we have seen, this formalism generally predicts more low-mass objects than PS. However, this is only true if the above mass dependence is less rapid than the PS value $M^{(n+D)/(2D)}$. Thus, if

$$f_{pk}(0) > \frac{n+D}{n+3D}, \tag{42}$$

then the low-mass part of the mass function will lie *below* that predicted by PS. The equality of the slope requires a mass larger than $(2\pi)^{3/2}\rho_0 R_f^3$ by only a moderate factor, 1.7 for $n=0$.

Comparing our mass functions with the simulations of Efstathiou *et al.* (1988) provides some encouragement for the peak models. For small $n$, the $N$-body functions undershoot the peak of the PS distribution by a factor $\sim 1.4$; the peak models which use the simple mass estimate undershoot by a larger factor than this, but the trend is qualitatively in the right direction. The $N$-body simulations at present lack the dynamic range to establish the low-mass slope directly, but simple considerations of probability tell us that there must be an excess of low-mass objects if there is a deficit around $M_*$.

In summary, if we believe that the appropriate mass to assign to a peak is indeed rather larger than the filter volume, the mass function may not be so different from the PS result. The theoretical grounds for such a choice are, however, hardly compelling; if the PS curve resembles what is seen in $N$-body simulations, this must look more than ever like a happy accident.

### 4.4 Numerical experiments

Given the approximate nature of some of the arguments we have used, it seems important to verify that they do provide a solution to the problems we have posed. Accordingly, we show in Fig. 4 the results of some Monte Carlo simulations, where the mass associated with each point has been evaluated explicitly by considering multiple filterings of a realization of a Gaussian field.

We considered one-dimensional arrays of $2^{16}$ points, and cubes of side $2^6$. The fields were then filtered (via FFT) by successive steps of 5 per cent in $R_f$ (smaller discrete increments in $\ln R_f$ produced essentially identical results). A running check was performed at each new filtering on whether a given grid point was associated with a collapsed object on that scale. This was defined by filtered $\delta > \delta_c$ for field points. For peaks, we required the point to be inside a volume $(2\pi)^{D/2} R_f^D$ centred on any peak with $\delta_{peak} > \delta_c$. The simulations were run until convergence in maximum mass occurred, typically for $\nu = 0.01$ – i.e. until the initial rms had been reduced by a factor $\gtrsim 300$. The results agree well with

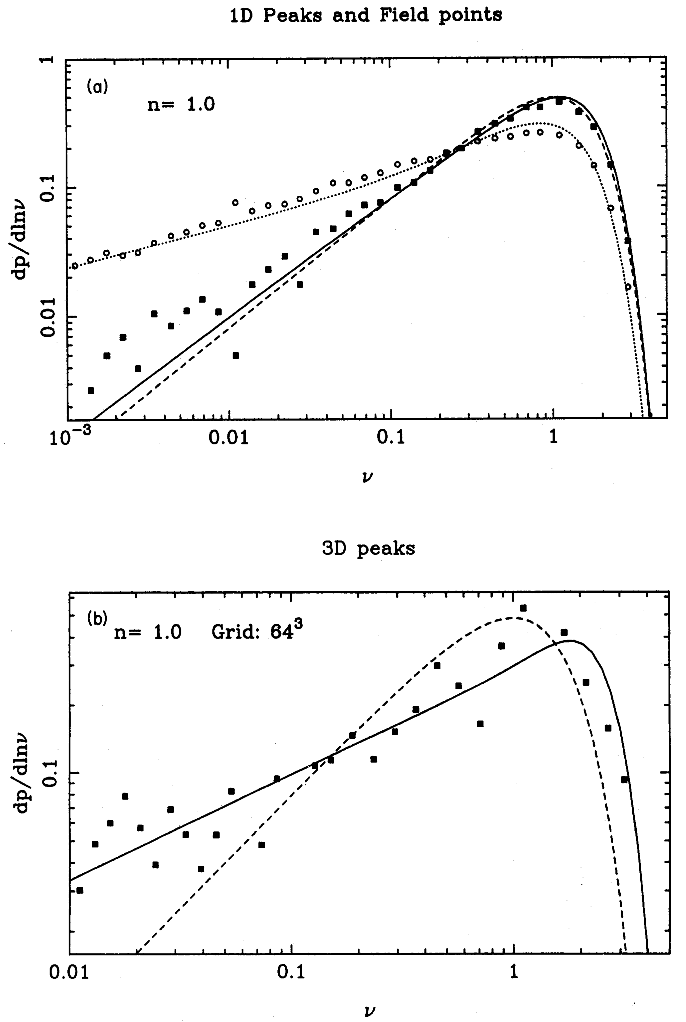


**Figure 4.** The results of our survival-probability ansatz compared to experiments on numerically generated Gaussian fields. (a) The one-dimensional results. The ansatz for peaks is shown as the full line, with the filled squares showing the numerical results. The circles are for field points, with the ansatz shown by the dotted curve. (b) The peaks mass function in three dimensions. The PS result is shown on both figures as a dashed line.

those calculated using our ansatz, although the 3D results are rather noisy.

## 5 COOLING AND THE GALAXY LUMINOSITY FUNCTION

Having discussed the mass functions for collapsed objects in a hierarchical universe, it is interesting to consider how these may relate to reality. The interpretation of the mass functions is straightforward when considering only 'haloes' of collisionless dark matter, but is more complex for baryonic matter, where we must ask if the matter has been able to *dissipate* and turn into stars. This question was analysed in a classic paper by Rees & Ostriker (1977), and has been reconsidered in the context of CDM by Blumenthal *et al.* (1984). Essentially, the point is that in the early universe, all forming structures *can* cool; a set of merging objects will create stars from the gas between them and subsequently will be identified as a single stellar system. Baryonic substructure can thus also be erased – unless star formation in the first generation of the hierarchy is so efficient that all gas immediately becomes locked up in compact clumps of stars. This seems implausible; the low binding energy should allow supernovae to unbind the matter (Dekel & Silk 1986), leading to a very low overall efficiency of star formation. Indeed, the high fraction of baryonic material in galaxy clusters, which is in the form of gas, may be indicative of such a process having taken place.

In order for dissipation to occur, however, the redshift of collapse clearly needs to be sufficiently large that there is time for an object to cool between its formation at redshift $z_{\rm cool}$ (when $\delta\rho/\rho \simeq \delta_{\rm c}$) and the present epoch. In other words, the mass exceeds $M$ if $\delta(M) > \delta_{\rm c}[1+z_{\rm cool}(M)]$. Once $z_{\rm cool}(M)$ is known, we can calculate the required *mass-dependent* threshold $\nu(M) = \delta_{\rm c}[1+z_{\rm cool}(M)]/\sigma_0(M)$ and insert this into equation (26). Section 5.1 calculates $z_{\rm cool}(M)$.

### 5.1 Collapse redshifts for effective cooling

The cooling function for a plasma in thermal equilibrium has been calculated by Raymond, Cox & Smith (1976). For an H + He plasma with $Y = 0.25$ and some admixture of metals, their results for the cooling time $[t_{\rm cool} \equiv 3kT/2\Lambda(T)n]$ may be approximated as

$$t_{\rm cool}({\rm yr}) = 1.8\times 10^{24}\left(\frac{\rho_{\rm B}}{M_\odot Mpc^{-3}}\right)^{-1}(T_8^{-1/2} + 0.5 f_{\rm m} T_8^{-3/2})^{-1}, \qquad (43)$$

where $T_8 \equiv T/10^8$ K. The $T^{-1/2}$ term represents bremsstrahlung cooling and the $T^{-3/2}$ term approximates the effects of recombination radiation. The parameter $f_{\rm m}$ governs the metal content; $f_{\rm m} = 1$ for solar abundances; $f_{\rm m} \simeq 0.03$ for no metals. In this model, where so far dissipation has not been considered, the baryon density is proportional to the total density, the collapse of both resulting from purely gravitational processes. $\rho_{\rm B}$ is then a fraction $\Omega_{\rm B}/\Omega$ of the virialized total density. This is itself some multiple $f_{\rm c}$ of the background density at virialization (which we refer to as 'collapse')

$$\rho_{\rm c} = f_{\rm c}\rho_0(1+z_{\rm c})^3. \qquad (44)$$

Using $\rho_0 = 2.78\times 10^{11}\Omega\, h^2\, M_\odot\, Mpc^{-3}$, we obtain

$$t_{\rm cool}/H_0^{-1} = 660(f_{\rm c}\Omega_{\rm B} h)^{-1}(1+z_{\rm c})^{-3}(T_8^{-1/2} + 0.5 f_{\rm m} T_8^{-3/2})^{-1}. \qquad (45)$$

The virialized potential energy for constant density is $3GM^2/(5r)$, where the radius satisfies $4\pi\rho_{\rm c} r^3/3 = M$. This energy must equal $3MkT/(\mu m_{\rm p})$, where $\mu = 0.59$ for a plasma with 75 per cent hydrogen by mass. Hence

$$T/K = 10^{5.1}(M/10^{12}M_\odot)^{2/3}(f_{\rm c}\Omega h^2)^{1/3}(1+z_{\rm c}). \qquad (46)$$

The criterion for formation of a galaxy by the present is that the cosmic time since $z_{\rm c}$ is some multiple $f_t$ of $t_{\rm cool}$ (for example, a spherical body in quasi-hydrostatic equilibrium has $f_t = 2$; Rees & Ostriker 1977). So, for $\Omega = 1$, we must solve

$$f_t t_{\rm cool} = \tfrac{2}{3}H_0^{-1}[1-(1+z_{\rm c})^{-3/2}]. \qquad (47)$$

If recombination cooling was important, the solution to this would be

$$(1+z_{\rm c}) = (1+M/M_{\rm cool})^{2/3}, \qquad (48)$$

where

$$M_{\rm cool}/M_\odot = 10^{13.1} f_t^{-1} f_{\rm m} f_{\rm c}^{1/2}\Omega_{\rm B}\Omega^{-1/2}. \qquad (49)$$

For high metallicity, where bremsstrahlung only dominates at $T \gtrsim 10^8$ K, this equation for $z_c$ will be a reasonable approximation up to $z_c \simeq 10$, at which point Compton cooling will start to operate. Given that we expect at least some enrichment rather early in the progress of the hierarchy, we shall keep things simple by using the above expression for $z_c$.

The effects of this cooling threshold on the mass function are illustrated in Fig. 5. At low masses, $z_{\rm cool} \simeq 0$ and the mass function is unaffected by cooling. At high masses, the cooling time is long for masses of order $M_c$, and $M^2 f(M)$ peaks at a much smaller mass. The sensitivity of this characteristic mass to $M_{\rm cool}$ is not very high; for $n=0$, it changes by a factor of ~ 10 when $M_{\rm cool}$ is altered by a factor of 100. Note that including bremsstrahlung makes little difference, because the virial temperature of the objects near the peak in $M^2 f(M)$ are below $10^8$ K. As the mass functions with and without cooling coincide for low masses, but given that cooling of massive objects is ineffective, probability in the mass function must accumulate at intermediate masses. Thus, the number of faint galaxies relative to bright is decreased. If $M_{\rm cool} \ll M_c$, then there is a power-law region between these two masses which differs from the PS slope; $M^2 f(M) \propto M^{[(n+3)/6]+(2/3)}$, i.e. there is an effective change in $n$ to $n+4$.

We should not claim too much from the above analysis, as several potentially important points are neglected. First, erasure of baryonic sub-structure may be imperfect, which would lead us to underestimate the numbers of low-mass objects (White & Rees 1978). Secondly, the criterion of equating cooling time with look-back time will work only if an object is able to cool undisturbed over this time; if subsequent generations of the hierarchy collapse while the object is still cooling quasistatically, then the gas will be reheated and collapse may never occur (see White & Rees for this point also). Objects are immune to this effect if the cooling time is shorter than the free-fall time, which turns out to be simply a criterion on mass (see e.g. Efstathiou & Silk 1983). If we relate collapse time $[t_{\rm coll} \equiv (3\pi/32 G\rho_c)^{1/2}]$ to cooling time via $f_t t_{\rm cool} = t_{\rm coll}$, then the above figures for recombination cooling yield a mass

$$M_{\rm coll}/M_\odot = 10^{13.5} f_t^{-1} f_m \Omega_B \Omega^{-1}. \tag{50}$$

This is of the same order as $M_{\rm cool}$, and so very massive structures may be truncated still more abruptly than we have assumed above.

Nevertheless, we feel that the qualitative point that cooling should lead to a steepening of the luminosity function, simply through probability conservation, is an important one. It is certainly a more appealing alternative than to postulate *ad hoc* variations in $M/L$ in order to reconcile the observed luminosity function with the PS low-mass slope.

## 6 APPLICATION TO CDM

We now illustrate the results of this paper for the 'standard' Cold Dark Matter spectrum (e.g. BBKS). This has an effective spectral index $n_{\rm eff}$ which increases with filter length. For galaxies, $n_{\rm eff} \simeq -2$, whereas for groups/clusters, $n_{\rm eff} \simeq 0$. The masses we quote may be converted into velocity dispersions, following Narayan & White (1988). Their calculation was based on the spherical model, for which virialization (collapse by a factor of 2 from maximum expansion) occurs at a density contrast with respect to the background of 176

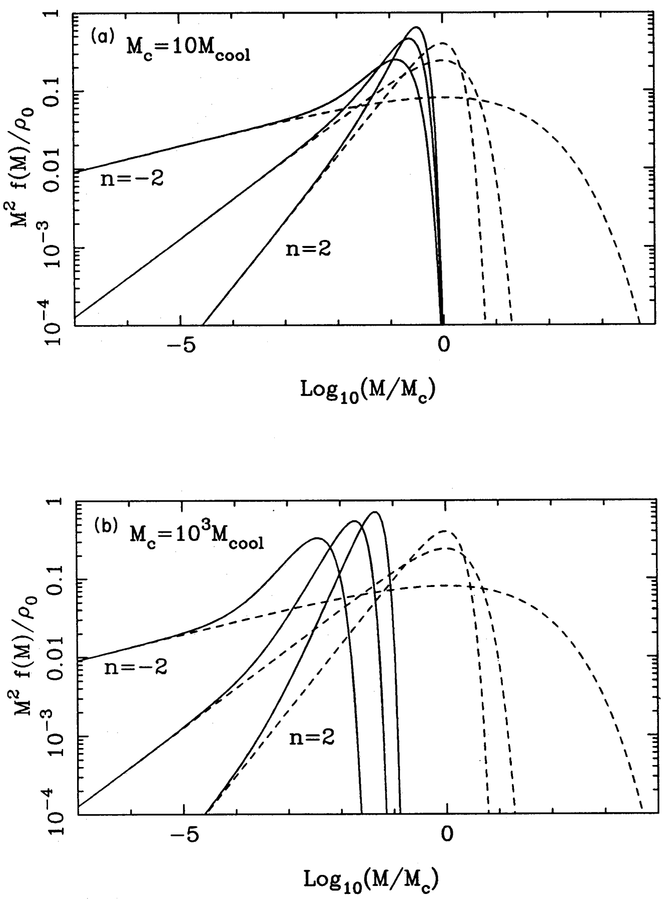


**Figure 5.** The mass functions resulting from the PS formalism with the adoption of the cooling threshold criterion $[\delta_c \to \delta_c (1+M/M_{\rm cool})^{2/3}]$. The solid lines show the mass functions with cooling, and the dashed lines show the mass functions without cooling; the two sets of curves coincide only at very low masses. $M_c$ is the mass scale with $\sigma(M_c) = \delta_c$.

Note (a) the relative insensitivity to $M_{\rm cool}$ and (b) that over several orders of magnitude in mass, the relative numbers of low-mass objects are greatly reduced by cooling.

(if $\Omega = 1$). The circular velocity of an orbit around such a body then follows as

$$V_c/{\rm km\,s^{-1}} = (M/10^{5.4} M_\odot)^{1/3} (1+z_v)^{1/2} \Omega^{-1/3} h^{1/3}, \tag{51}$$

for virialization at redshift $z_v$. In practice, a virialized system will tend to relax towards the isothermal sphere, for which the velocity dispersion is $\sigma_v = V_c/\sqrt{2}$. This relation is quite robust, as it depends on only the $\frac{1}{6}$th power of the virialized density contrast.

The mass functions for CDM depend on the normalization of the power spectrum. The most common method is via the integral over the correlation function, $J_3(10\,h^{-1}\,{\rm Mpc}) = 270\,h^{-3}\,{\rm Mpc}^3$ (Davis & Peebles 1983), as this is rather insensitive to non-linear corrections. This yields results very similar to those obtained by requiring the linear-theory rms to be unity in spheres of radius $8\,h^{-1}$ Mpc. One must also specify a bias factor, $b$, and Hubble parameter $h$. Since the CDM spectrum is not a power law, these parameters may not be factored out in a simple way. However, to avoid complication, we show results for one set of parameters, designed to be in the middle of the commonly discussed range. The effects of varying these parameters is not

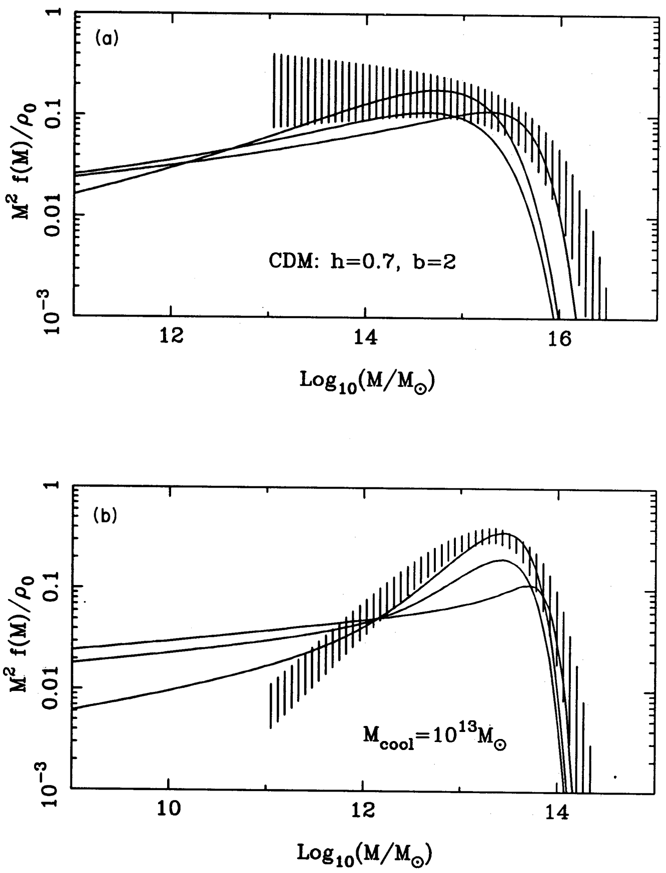


**Figure 6.** The predicted mass functions for CDM, using Gaussian filtering with $M=(2\pi)^{3/2}\rho_0 R_f^3$ and $\delta_c=1.69$. (a) The mass function for 'haloes'. Working from the right at the high-mass end, the three solid curves show the peak ansatz, PS, and the ansatz for field points. The hatched area is the group multiplicity function from Bahcall (1979). (b) The same as (a) but for 'cooled' objects. The hatched area is the fit to the galaxy luminosity function from Efstathiou, Ellis & Peterson (1988), with a closure mass-to-light ratio.

vast, and can in any case be approximately inferred by comparison with power-law spectra. We adopt $h=0.7$, $b=2$, $M_{\rm cool}=10^{13}M_\odot$.

The result for the various mass functions we have considered, with and without cooling, is shown in Fig. 6. These curves assume $\delta_c=1.69$.

### 6.1 Comparison with luminosity functions

For comparison with observation, consider the galaxy and cluster luminosity functions in Schechter form

$$\phi=\phi^*\left(\frac{L}{L^*}\right)^{-\alpha} e^{-L/L^*}\frac{dL}{L^*}. \tag{52}$$

The corresponding luminosity density is $\phi^* L^* \Gamma(2-\alpha)$. Comparison with the background density of $2.78\times10^{11}\Omega h^2 M_\odot\ {\rm Mpc}^{-3}$ gives the equivalent of $L^*$ in mass

$$M^*=\frac{\rho_0}{\phi^*\Gamma(2-\alpha)}. \tag{53}$$

For galaxies, we take $\alpha=1.07$, $\phi^*=0.0156\ h^3$, from Efstathiou, Ellis & Peterson (1988), which yields $M^*=10^{13.2}\Omega\ h^{-1}M_\odot$. Although this value assumes constant $M/L$, it may be thought of as the effective total mass corresponding to an $L^*$ galaxy, as these dominate the luminosity density. This is a huge mass, and certainly should not be thought of as being potentially observable. It does, however, correspond directly to the total halo masses one considers in the PS formalism, because all the mass is assigned to one object or another.

For groups/clusters, Bahcall (1979) found $\alpha=2$, $\phi^*=1.3\times10^{-5}h^3$ and $L^*=2.5\times10^{12}h^{-2}L_\odot$. Here, the total luminosity density is formally divergent. However, the group function matches on to the galaxy function, so we may integrate only down to the galaxy $L^*$. This yields a luminosity density of $10^{8.2}hL_\odot\ {\rm Mpc}^{-3}$, which is close to the total obtained from galaxies. The group function accounts for all the light, just as our $f(M)$ accounts for all the mass, and we therefore adopt the closure $M/L$ value deduced from the galaxy luminosity function in order to deduce the group $f(M)$. There is an inconsistency here in the treatments of some authors (e.g. Colafrancesco, Lucchin & Matarrese 1989), who apply observed $M/L$ ratios ($\sim 300\,h$) to convert between luminosity functions and mass functions. This is not consistent with $\Omega=1$; integration under their mass functions will produce an incorrect total density. The existence of bias must mean in practice that clusters, like galaxies, have dark haloes. The PS formalism deals with the total mass, and so observed $M/L$ ratios from the centres of clusters are not relevant.

In practice, the comparison with observation shown in Fig. 6 is reasonably encouraging. The characteristic masses can be reproduced to within uncertainties imposed by possible variations in $\delta_c$, $M(R_f)$ and $M_{\rm cool}$, and the shape of the mass functions is not unreasonable given realistic uncertainties in the data. The slope of the galaxy luminosity function is particularly interesting. The observed range of low-mass slopes for the galaxy luminosity function is in the range 0–0.25, which apparently requires $1.5<n<3$ on galaxy scales according to the basic PS result. With our simple cooling prescription of $n\rightarrow n-4$, this becomes well consistent with the sort of index expected from CDM ($-2\lesssim n\lesssim -1$).

## 7 SUMMARY

We have tried to analyse in detail the distribution of masses expected for collapsed objects in a hierarchical universe. We believe we have exposed more clearly some of the conceptual problems associated with the Press–Schechter analysis, and shown how to solve correctly the original Press–Schechter problem. We have also dealt with an improved version of the analysis, which takes into account the changes involved in imposing the peak constraint. The method allows further criteria for formation of structures to be imposed. We illustrate this by adding the criterion that a 'luminous' object must have had time to cool. We thus obtain a mass function for luminous objects which differs markedly from that of the dark 'haloes'.

Our main conclusion is that there is no good justification for adopting a mass function of the Press–Schechter form, and in particular that the low-mass slope may well be different. The predicted mass function depends on the form of filter function one uses, and on the precise peak mass estimate adopted, both of which can make substantial differences to the slope of the mass function. A similar problem concerning the effect of filter choice was encountered by Lumsden, Heavens & Peacock (1989) in their analysis of the clustering of density peaks. These difficulties illustrate the limitations of linear theory in tackling problems of this sort.

Nevertheless, we believe that these analytic tools are in principle very useful, not least in helping us to understand the results of N-body simulations. Further progress in this area now requires calibration against non-linear numerical studies of large dynamic range.

## ACKNOWLEDGMENTS

Conversations with Dick Bond, Sean Cole, Nick Kaiser and Simon White helped develop our ideas on this subject. JAP also thanks the Canadian Institute for Theoretical Astrophysics for their hospitality while part of this work was carried out. An unpublished 1987 preprint by Barbara Ryden gave us the idea of using cooling to obtain a mass-dependent threshold.

## REFERENCES

Bahcall, N. A., 1979. *Astrophys. J.*, **232**, 689.
Bardeen, J. M., Bond, J. R., Kaiser, N. & Szalay, A. S., 1986. *Astrophys. J.*, **304**, 15 (BBKS).
Blumenthal, G. R., Faber, S. M., Primack, J. R. & Rees, M. J., 1984. *Nature*, **311**, 517.
Bond, J. R., 1989. *Large-Scale Motions in the Universe*, Proc. Vatican Study Week, p. 419, eds Rubin, V. C. & Coyne, G. V., Princeton University Press, New Jersey.
Bond, J. R. & Efstathiou, G., 1987. *Mon. Not. R. astr. Soc.*, **226**, 655.
Carlberg, R. G. & Couchman, H. M. P., 1989. *Astrophys. J.*, **340**, 47.
Chandrasekhar, S., 1943. *Rev. Mod. Phys.*, **15**, 1. Reprinted in *Selected Papers on Noise and Stochastic Processes*, p. 3, ed. Wax, N., Dover, New York.
Colafrancesco, S., Lucchin, F. & Matarrese, S., 1989. *Astrophys. J.*, **345**, 3.
Davis, M. & Peebles, P. J. E., 1983. *Astrophys. J.*, **267**, 465.
Dekel, A. & Silk, J., 1986. *Astrophys. J.*, **303**, 39.
Efstathiou, G. & Rees, M. J., 1988. *Mon. Not. R. astr. Soc.*, **230**, 5P.
Efstathiou, G. & Silk, J., 1983. *Fundam. Cosmic Phys.*, **9**, 1.
Efstathiou, G., Ellis, R. S. & Peterson, B. A., 1988. *Mon. Not. R. astr. Soc.*, **232**, 431.
Efstathiou, G., Frenk, C. S., White, S. D. M. & Davis, M., 1988. *Mon. Not. R. astr. Soc.*, **235**, 715.
Heavens, A. F. & Peacock, J. A., 1988. *Mon. Not. R. astr. Soc.*, **232**, 339.
Lucchin, F. & Matarrese, S., 1988. *Astrophys. J.*, **330**, 535.
Lumsden, S. L., Heavens, A. F. & Peacock, J. A., 1989. *Mon. Not. R. astr. Soc.*, **238**, 293.
Narayan, R. & White, S. D. M., 1988. *Mon. Not. R. astr. Soc.*, **231**, 97P.
Peacock, J. A. & Heavens, A. F., 1985. *Mon. Not. R. astr. Soc.*, **217**, 805.
Press, W. H. & Schechter, P., 1974. *Astrophys. J.*, **187**, 425 (PS).
Raymond, J. C., Cox, D. P. & Smith, B. W., 1976. *Astrophys. J.*, **204**, 290.
Rees, M. J. & Ostriker, J. P., 1977. *Mon. Not. R. astr. Soc.*, **179**, 541.
Rice, S. O., 1954. *Mathematical Analysis of Random Noise. In Selected Papers on Noise and Stochastic Processes*, p. 133, ed. Wax, N., Dover, New York.
White, S. D. M. & Rees, M., 1978. *Mon. Not. R. astr. Soc.*, **183**, 341.